Structural Engineering and Mechanics, *Vol. 53, No. 2 (2015) 189-204*
DOI: http://dx.doi.org/10.12989/sem.2015.53.2.189

Experimental characterization of timber framed masonry walls cyclic behaviour

Ana Maria Gonçalves*, João Gomes Ferreira[a], Luís Guerreiro[b] and Fernando Branco

Department of Civil Engineering, Technical University of Lisbon from University of Lisbon,
Lisbon 1049-001, Portugal

(Received June 14, 2013, Revised April 16, 2014, Accepted April 27, 2014)

Abstract. After the large destruction of Lisbon due to the 1755 earthquake, the city had to be almost completely rebuilt. In this context, an innovative structural solution was implemented in new buildings, comprising internal timber framed walls which, together with the floors timber elements, constituted a 3-D framing system, known as "cage", providing resistance and deformation capacity for seismic loading. The internal timber framed masonry walls, in elevated floors, are constituted by a timber frame with vertical and horizontal elements, braced with diagonal elements, known as Saint Andrew's crosses, with masonry infill.
This paper describes an experimental campaign to assess the in-plane cyclic behaviour of those so called "frontal" walls. A total series of 4 tests were conducted in 4 real size walls. Two models consist of the simple timber frames without masonry infill, and the other two specimens have identical timber frames but present masonry infill. Experimental characterization of the in-plane behaviour was carried out by static cyclic shear testing with controlled displacements. The loading protocol used was the CUREE for ordinary ground motions. The hysteretic behaviour main parameters of such walls subjected to cyclic loading were computed namely the initial stiffness, ductility and energy dissipation capacity.

Keywords: "Pombaline" buildings; cyclic loading tests; earthquake

1. Introduction

Timber framed masonry wall buildings are seen all over Europe, especially in seismic regions, given its adequacy to resist earthquake (Diskaya 2007, Dogangun *et al.* 2006, Dutu *et al.* 2012, Gulkan 2004, Langenbach 2007, Makarios and Demosthenous 2006, Redondo *et al.* 2003). The "pombaline" buildings, named after the Marquis of Pombal, in particular, present a structure with maximum of four storeys, with arcades at the ground floor, masonry facade walls and internal timber framed masonry walls. These walls, together with the floors' timber beams, form the 3-D cage that constitutes the seismic resistant structure (Fig. 1). The Marquis of Pombal ordered their construction after the 1755 earthquake that destroyed Lisbon, aiming at providing the city with seismic resistant buildings (Ferreira *et al*. 2012).

*Corresponding author, Ph.D. Student , E-mail: goncalves.amn@gmail.com
[a]Professor, E-mail: joao.gomes.ferreira@ist.utl.pt
[b]Professor, E-mail: luisg@civil.ist.utl.pt

http://www.techno-press.org/?journal=sem&subpage=8 ISSN: 1225-4568 (Print), 1598-6217 (Online)

Fig. 1 Timber framed wall in "pombalino" building (Gonçalves *et al.* 2011)

In traditional half-timbered building, it is usual that half-timbered walls are also placed in parallel to external gravity load bearing masonry walls. In unreinforced masonry structures, the capacity of the building is good in terms of vertical loads, since masonry has generally an adequate compressive strength. When subjected to horizontal loads, though, shear and flexural capacity of such structures are quite low, particularly vulnerable to out–of-plane failure mechanisms. When a bracing system is added, the lateral resistance increases, improving the seismic behavior of the structure. The internal half-timbered walls represent the lateral load bearing walls of the structure, since due to their lightness and higher flexibility than traditional masonry walls, they are expected to perform better under seismic loads. The timber-framed masonry walls are connected to the external masonry walls by means of the timber floor beams, which are connected both to the timber-framed and to the external masonry walls. This system can be also beneficial to reduce the out-of-plane vulnerability of masonry walls.

In some recent earthquakes (Turkey 1991, Greece 003, India 2005) half-timbered building showed a better behviour than unreinforced masonry buildings (Langenbach 2007). In fact, this construction system is pointed out by several authors as one of the most efficient earthquake resistant structure in the world (Langenbach 2007 and Makarions *et al*. 2006), but their popularity is not only due to their seismic performance, but also to their low cost and the strength they offer.

Though the "Pombalino" buildings have a good anti-seismic design, after more than 250 years rehabilitation works are required, mainly, due to degradation and inadequate interventions (e.g., adding storeys, modifying structural elements or changing the functionality of the building). Also, the new codes establish more demanding rules regarding earthquake resistance.

This particular type of walls has already been the focus of a few laboratory tests. In the work of Santos (Santos 1997, Santos 1999) three walls extracted from a real building were tested in quasi-static cyclic conditions, by imposing displacements at the top of the wall. Nevertheless, no vertical loads were applied to simulate the effect of the dead loads from the adjacent floors. These tests had the benefit of using real walls although some damage might have occurred during removal and transportation to the test facility, which could have affected the behavior of the walls. Furthermore the simulation of the in situ base constraints in the extremities was also difficult to ensure.

A similar experimental campaign was conducted by Meireles and Bento (2010) where three newly constructed walls were tested in static cyclic conditions. The design of these walls was intended to be a faithful replica of the original ones, by replicating the geometry, materials and construction techniques as much as possible. Although different types of timber were usually used in the construction of these walls, such as oak or chestnut, pine timber was adopted as it is also common and it is in abundance as a current construction material (Meireles and Bento (2010). Forged steel nails were used in the connections between timber elements according to traditional configurations. The filling was adopted as broken bricks and tiles, connected by a hydraulic lime mortar. The walls were subjected to cyclic displacements applied on the top with increasing amplitude, until failure.

Some numerical works available in literature considers the evaluations of the seismic vulnerability of Pombalino masonry buildings, consisted the contribution of the timber-framed masonry walls (Bento *et al*. 2005). Other works were carried out on Pombalino buildings as a whole, without the internal cage “gaiola” structure. These studies analyzed numerically a model consisting only of the exterior masonry walls to assess the ‘‘block effect’’ of structural interventions made on historical buildings, i.e., the global effect that these interventions had on the neighbourhood (Coias *et al*. 2001).

The present work is included on the ongoing project “REABEPA” (i.e., Structural Rehabilitation of Masonry Walls in Old Buildings), which main purpose is to study the structural strengthening techniques available to reinforce in masonry walls typologies, since they have to be preserved due to the significant cultural heritage in many countries (e.g., Portugal, Turkey, Greece, Italy, India). Due to the nature of an earthquake, cyclic and dynamic loadings are studied to better understand the behavior of the walls, with and without reinforcements. The masonry importance in the structural behavior of the walls is also discussed in this paper and these results are very useful and essential for further analytical work in modeling the non-linear behaviour of such walls.

2. Experimental program

This work is experimental based and it aims at getting a better insight on the cyclic behaviour of traditional timber framed masonry walls tested under static loads, in order to assess its advantages in seismic regions, and to contribute to the state of the art on this issue. A brief description of the wall specimens and of the test procedures is presented next.

2.1 Objectives

The objective of the experimental work developed and presented herein is to obtain the cyclic behaviour of the timber framed masonry walls through static cyclic shear testing under controlled displacements. Simple timber frames (without masonry infill) were also tested to assess the contribution of these frames to the overall behaviour of the timber-masonry wall.

The experimental work on timber framed walls comprised two parts. The first part consisted of a campaign to assess the in-plane seismic behavior of timber framed masonry walls and to evaluate the effect of its components (timber frame, masonry) (Figs. 2(a)-(b)). The second parte aimed at evaluating the adequacy and efficacy of three proposed seismic rehabilitation methods based on buckling restrained damping braces, steel plate reinforcement on timber elements connections and reinforced plaster. In this paper only the first part of the experimental campaign will be presented.

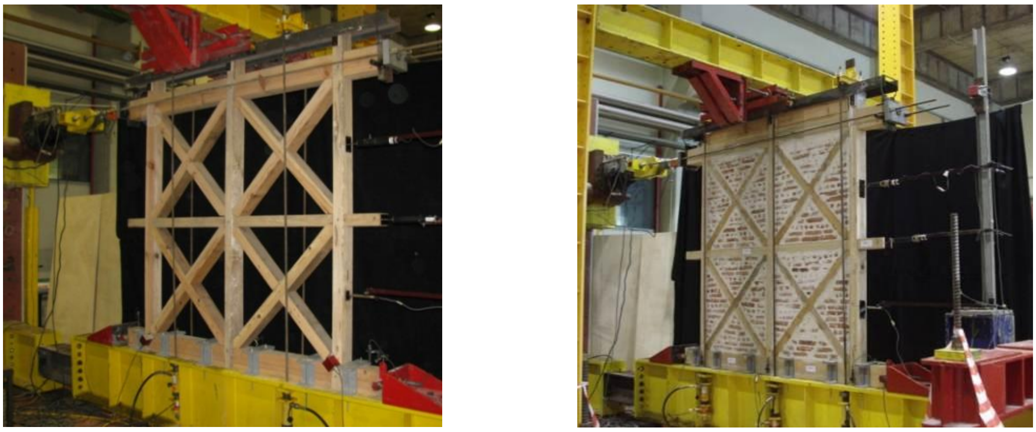

(a) Timber frame (TF) specimen (b) Masonry wall (MW) specimen

Fig. 2 Tested specimens

Fig. 3 Crosshaving joints

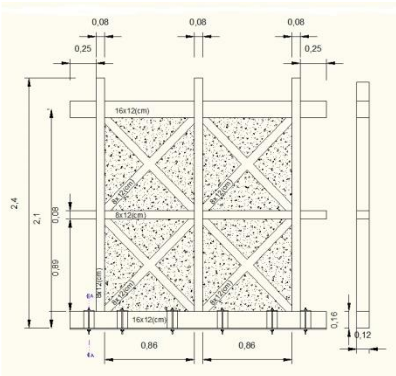

Fig. 4 Model's dimensions (m)

Fig. 5 Masonry wall fabrication

2.2 Tested specimens

The tested specimens present four Saint Andrew's crosses each. Two models consist of the simple timber frames without masonry infill, referred to as "timber frames - TF" (Fig. 2(a)). The other two specimens have identical timber frames but present masonry infill and are referred to as "masonry walls - MW" (Fig. 2 (b)).

Cross-halving joints (illustrated in Fig. 3) were used in the connections between vertical and horizontal timber elements and between the crossing diagonals. The connections between the diagonals and their end nodes were obtained by simply sawing them at 45º. All connections were reinforced with iron nails. The wood used in the experimental study was stone pine (pinus pinea) class C18 (EN 338, 2003). The wood sections were 16×12 cm^2 (base and top beam) and 8×12 cm^2 (all other elements). Fig. 4 shows the dimensions of the timber frame wall.

The choice of the type of masonry was very important since there are several types of infill, including mortar with bricks or mortar with tiles or even mortar mixed with small stones. In this study, mortars with bricks (Fig. 5) were used. The masonry consists of bricks and cement-lime-sand mortar with a volume ratio of 1:2:6 (hydrated lime: portland cement 32.5 N: sand). Although

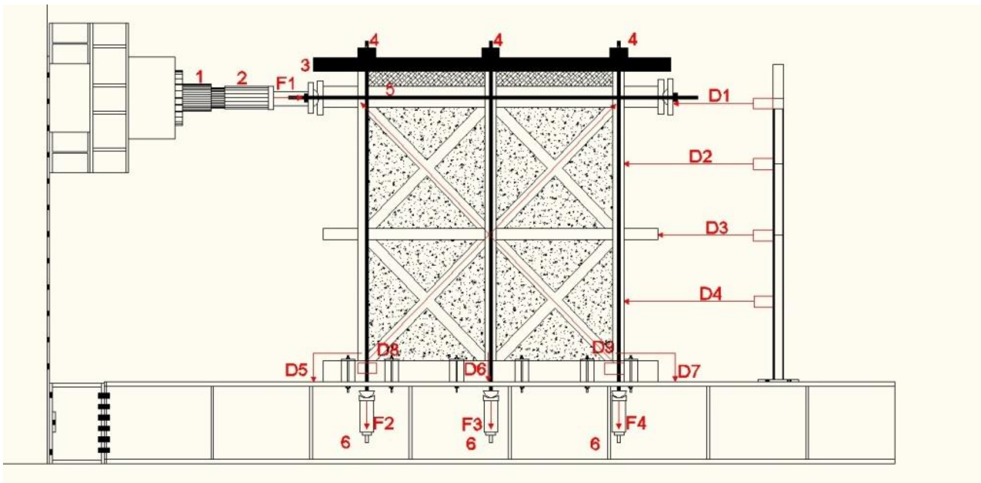

Legend: 1) Actuator; 2) Load Cell; 3) Load distribution beam; 4) Prestressing rods; 5) Wooden beam 6) hydraulic jacks; D1 to D8) displacement transducers

Fig. 6 Test set-up

ancient mortars were solely composed of lime and sand, cement was added in these cases to ensure a faster cure. The drying time was two months.

2.3 Experimental procedures

A series of quasi-static tests were performed in the reaction wall at the Laboratory of Structures and Strength of Materials of the Instituto Superior Técnico. The tests involved the application of horizontal and vertical load on the models. The walls were tested under a constant vertical load and a controlled horizontal displacement applied at the top of the wall by a 400 mm stroke actuator with 1000 kN capacity.

The walls were fully instrumented to measure the displacement at different points. The general layout of the equipment is shown in Fig. 6. The displacement transducers D1 to D4 measured the horizontal displacement on the wall at different heights, D5 to D7 measured the vertical lift of the vertical timber element in regard to the bottom wood beam, D8 and D9 measured the displacement in the diagonals. The load imposed by the actuator was also measured with a load cell, as well as the force in the vertical cables used to impose the vertical load.

To prevent the masonry wall from rocking, the bottom wooden beam was bolted to a base steel beam at six fixation points. The out-of-plane motion was prevented with lateral rollers at the top.

The test procedure consisted of imposing a cyclic horizontal displacement at the top. A constant vertical load was transmitted at the top of the elements to simulate gravity loads with six steel cables tensioned with hydraulic jacks. The vertical loading to impose on the test structure was determined based on EN 1991-1 (CEN, 2002) and is given by Eq. (1). It was considered that the wall was placed at the first floor of a three story building plus ground floor. The area of influence of the walls was considered to be of 5 m^2. The total vertical load applied to the masonry wall was then estimated as 30 kN/m.

$$S_d = S_w + 0.3 \times L_L \tag{1}$$

Table 1 Caption

Segment	N° of cycles	Amplitude in the primary cycle (%)×Δ
1	6	5% ×Δ
2	7	7.5% ×Δ
3	7	10% ×Δ
4	4	20% ×Δ
5	4	30% ×Δ
6	3	40% ×Δ
7	3	70% ×Δ
8	3	100% ×Δ
9	3	(100% + 100% ×α) ×Δ
10	3	(100% + 2×100% ×α) ×Δ

Where S_d is the vertical loading, S_W is the self-weight, L_L is the live load.

2.4 Loading protocol definition

Experimental characterization of the in-plane behaviour was carried out by static cyclic shear testing with controlled displacements, as referred. The loading protocol used was the CUREE (Krawinkler 2000, EN 1015 1999). This protocol consists of cyclic displacement sequences increasing in amplitude (α) throughout the test, each segment consisting of a primary cycle, with the amplitude defined as a multiple of the reference displacement (Δ), followed by a series of cycles with amplitude equal to 75% of the primary cycle (Table 1).

In the case study It was used the reference value (D) of 90 mm. This reference value was obtained at an experimental test formerly performed at IST by Meireles (2010), due to the characteristics of the tests were similar. With this procedure it was avoided the construction of an additional specimen.

3. Result

3.1 Timber Frames (TF)

The load-displacement diagrams obtained for the timber frames (TF) are shown in Fig. 7. The cyclic displacements were increased until rupture. An increase in the walls stiffness, occurring for displacement higher than about 60 mm, was identified in the load-displacement diagrams. However, this boost in the wall stiffness is due to the increase of strength in the tensioned cables jacks, when they reach their limit course and start to behave as tie rods. Due to this behaviour, these values cannot be taken into account for the characterization of the walls. The analysis is limited to a range of imposed displacements ±55 mm, which corresponds to a significant drift of 2.6%.

The hysteretic behaviour of the “frontal” walls subjected to cyclic loading is characterized by nonlinear behaviour with a high ductility response. The maxim strength is 30 kN for the timber frame walls, measured at the displacement of 55 mm (2.6% drift).

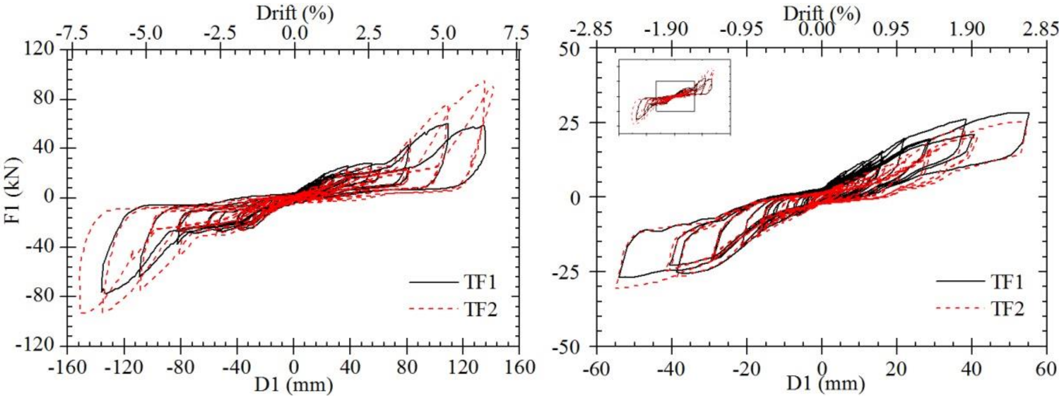

Fig. 7 Force-Displacement curves of timber frames

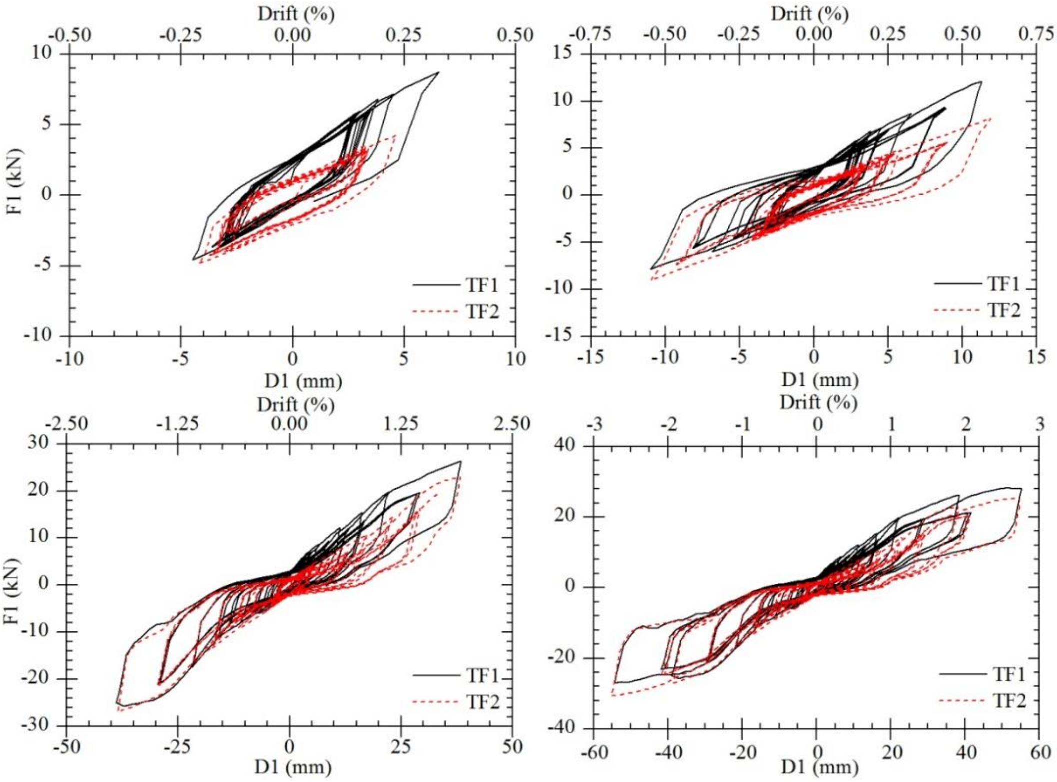

Fig. 8 Force-displacement curves of timber frames along the displacement history

As shown in Fig. 8, in the first cycles the timber frame walls present practically bilinear behaviour, up to approximately 12 mm (0.5% drift). As displacements increase, a number of effects such as cracking and yielding or degradation of stiffness became more visible.

The extremities of the load-displacement hysteresis loops are envelope curves. The envelope curve contains the peak loads of the first cycle of each segment of the cyclic loading. Wall displacement in the positive direction produces a positive envelope curve; the negative wall

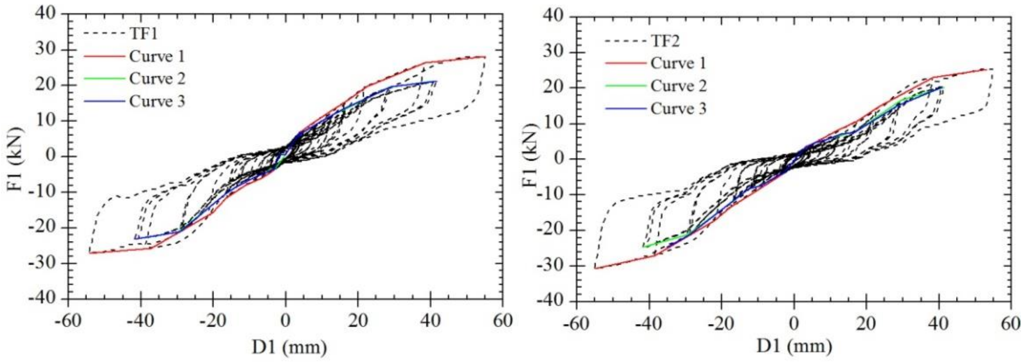

Fig. 9 Load-displacement envelope curves

Table 2 Wall stiffness

TF1	F_{max} (kN)	F_{min} (kN)	$\lvert F_{ave}$ (kN)$\rvert$	$v_{40\%Fmax}$ (mm)	$v_{40\%Fmin}$ (mm)	$v_{40\%Fave}$ (mm)	$v_{10\%Fmax}$ (mm)	$v_{10\% Fmin}$ (mm)	$v_{10\% Fave}$ (mm)	k (kN/m)
1ª curve	28.2	-27.0	27.6	12.3	-15.4	13.9	1.1	-2.8	2.0	696.0
2ª curve	21.1	-22.8	21.9	8.7	-13.7	11.2	0.9	-2.8	1.9	703.6
3ª curve	21.3	-21.0	21.2	8.5	-13.7	11.1	0.9	-2.8	1.9	686.6
TF2	F_{max} (kN)	F_{min} (kN)	$\lvert F_{ave}$ (kN)$\rvert$	$v_{40\%Fmax}$ (mm)	$v_{40\%Fmin}$ (mm)	$v_{40\%Fave}$ (mm)	$v_{10\%Fmax}$ (mm)	$v_{10\% Fmin}$ (mm)	$v_{10\% Fave}$ (mm)	K (kN/m)
1ª curve	25.2	-30.7	27.9	18.2	-14.3	16.2	2.7	-1.7	2.2	598.2
2ª curve	20.3	-24.7	22.5	18.1	-13.5	15.8	2.3	-1.7	2.0	488.7
3ª curve	20.1	-24.6	22.4	18.0	-13.2	15.6	2.2	-1.7	2.0	492.5

displacement produces a negative envelope curve.

According to ISO 21581 (2009), the first, second and third envelope curves for the cyclic tests shall be established by connecting the points of maximum load in the hysteresis plot in each displacement level in the first, second and third reversed cycles, respectively (Fig. 9).

Properties such as stiffness, yield displacement, ductility and impairment of strength can be determined from the envelope curves according to the definitions adopted.

Stiffness may be calculated by Eq. (2) for the first, second and third envelope curves of the cyclic test specimens. Parameters v40%Fmax and v10%Fmax in Eq. (2) are the displacement values obtained at 40% and 10% of maximum load (F_{max}), respectively, for the envelope curves.

$$K = \frac{0.3 \times F_{max}}{\upsilon_{40\% F_{max}} - \upsilon_{10\% F_{max}}} \tag{2}$$

Accordingly, based on the values presented in Table 2, the stiffness of the wall was estimated in 694 kN/m for TF1 specimen and in 526 kN/m for TF2 specimen (average of three curves). This difference could be related with the behaviour of timber connections and with the heterogeneity in material properties.

The energy dissipated in each cycle may be evaluated by calculating the area within the load-displacement curve in each cycle. Fig. 10 and Table 3 show the behaviour of load - displacement of the walls along the cycles, where a decrease in damping with increasing imposed deformation can be observed. The damping coefficient for a given cycle may be estimated based on the following equation

$$\zeta = \frac{E_d}{2\pi \times F_{max} \times d_{max}} \tag{3}$$

In Eq. (3), the dissipated energy, E_d, corresponds to the area of the graph delimited by the cycle, F_{max} is the maximum force measured on the structure during that cycle and d_{max} is the maximum deformation in the structure during that cycle.

The energy dissipation per cycle associated with the hysteretic behaviour of the wall was determined by measuring the area of the wider cycle in each stage of deformation in the force-displacement diagram. In Table 3 the energy dissipated in cycles at different levels of deformation is presented. The increase in deformation leads to a higher increase in energy dissipation and less damping, associated to damage in the wooden beams.

The load was increasing with the imposed displacement until the rupture of one diagonal element, which occurred, associated with lateral instability. Fig. 11 shows the failure modes of timber frames.

3.2 Masonry walls (MW)

Two masonry walls, MW1 and MW2, constituted by a timber frame with masonry infill, were

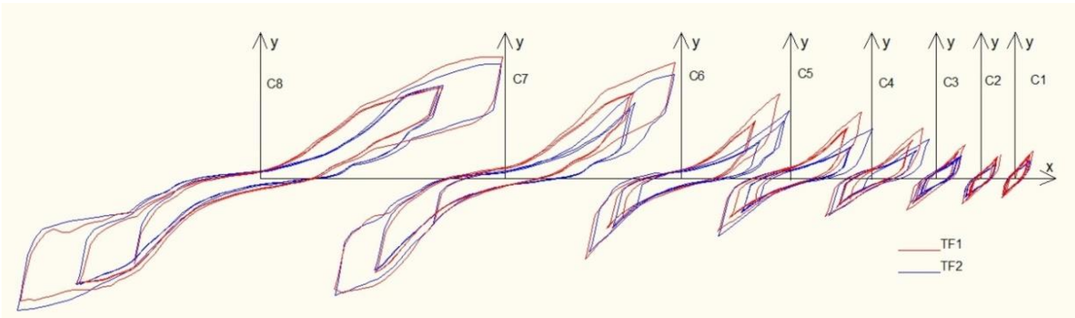

Fig. 10 Load-displacement envelope curves Energy dissipated in each cycle

Table 3 Energy dissipated and damping coefficient in each cycle

Cycle	TF1						TF2					
	D_{max} (mm)	F_{max} (kN)	F_{min} (kN)	F_{ave} (kN)	E (kN.mm)	ζ (%)	D_{max} (mm)	F_{max} (kN)	F_{min} (kN)	F_{ave} (kN)	E (kN.mm)	ζ (%)
C1	3.83	6.84	-3.63	5.23	19.75	15.69	3.30	3.58	-4.02	3.80	15.38	19.52
C2	4.54	7.18	-4.57	5.88	26.35	15.70	4.63	4.22	-4.84	4.53	17.70	13.42
C3	6.57	8.72	-6.02	7.37	48.74	16.01	5.90	4.86	-5.68	5.27	32.40	16.59
C4	11.30	12.14	-7.88	10.01	111.03	15.63	11.91	8.18	-9.06	8.62	99.90	15.49
C5	16.28	15.45	-11.60	13.53	181.15	13.09	17.46	10.75	-13.51	12.13	181.87	13.67
C6	22.26	19.76	-17.50	18.63	270.68	10.39	23.23	14.65	-17.25	15.95	253.25	10.88
C7	38.48	26.30	-25.79	26.04	721.08	11.45	38.36	23.04	-27.01	25.02	641.67	10.64
C8	55.24	28.21	-27.01	27.61	1138.03	11.88	54.83	25.22	-30.65	27.94	1071.00	11.13

(a) Failure by compression and lateral instability of diagonal in TF1

(b) Failure by compression and lateral instability of diagonal in TF2

Fig. 11 Failure mode of timber frames

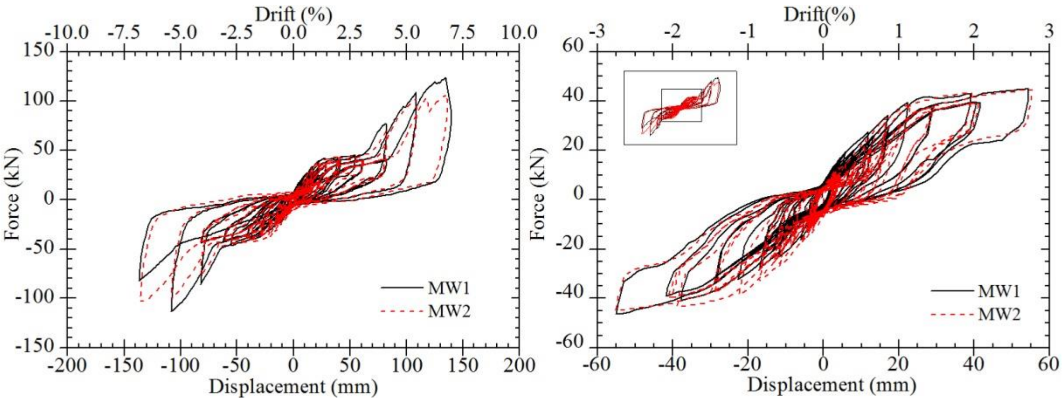

Fig. 12 Force-displacement curves

submitted to the same displacement history as the timbre frames (TF).

Fig. 12 shows load-displacement diagrams, presenting an increase in the wall stiffness for displacements higher than 60 mm due to the increase of load in the jacks, as occurred in the TF specimens. Due to this behaviour, these values cannot be taken into account for the characterization of the walls and the analysis is limited to a range of ±55 mm displacements, which results in a 2.6% drift. The maximum strength within this cycles' amplitude is 50 kN, measured at the displacement of 55 mm, corresponding to a significant drift of 2.6%.

The results presented on Fig. 13 show two distinct behaviour types. In the first cycles the walls present practically linear behaviour, up to approximately 35 kN and 15 mm (0.7% drift). The small hysteresis loops in this phase are associated to gaps in the connections, which open and close according to the direction of the load. As displacement increases, a number of effects that characterize the nonlinear behaviour become visible around 45 kN load and 55 mm displacement which results in a 2.6% drift.

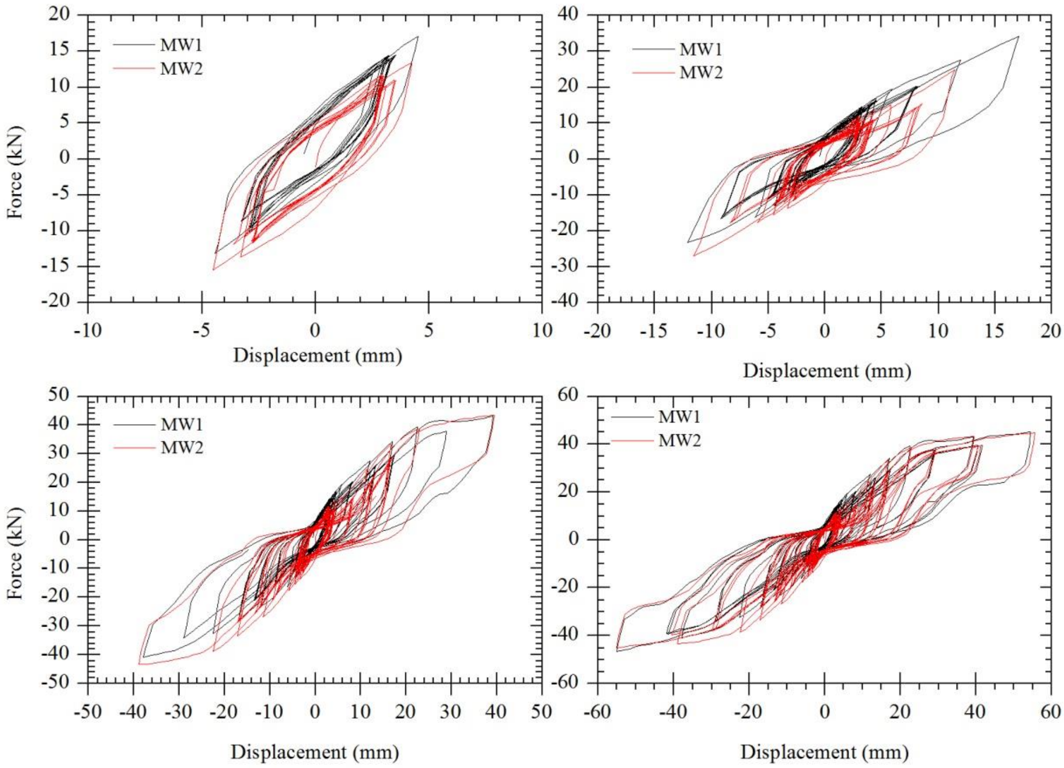

Fig. 13 Force-displacement curves of masonry walls along the displacement history

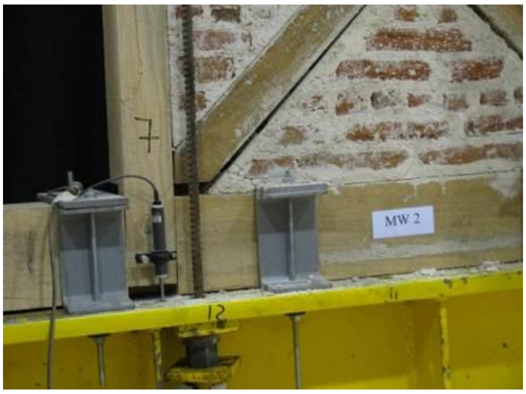

Fig. 14 Vertical lift of bottom beam and vertical member

A certain vertical lift of the bottom beam occurred during the wall test, as well as a separation of the vertical timber elements from the bottom beam, as an effect of a rocking movement that was not eliminated, becoming more significant with the increase of the overall deformation (Fig. 14).

The curves shown in Fig. 15 correspond to the evolution of hysteretic behaviour of the walls MW1 and MW2 that showed an identical behaviour. According to ISO/DIS 21581, stiffness properties are determined by the envelope curves based on Eq. (2).

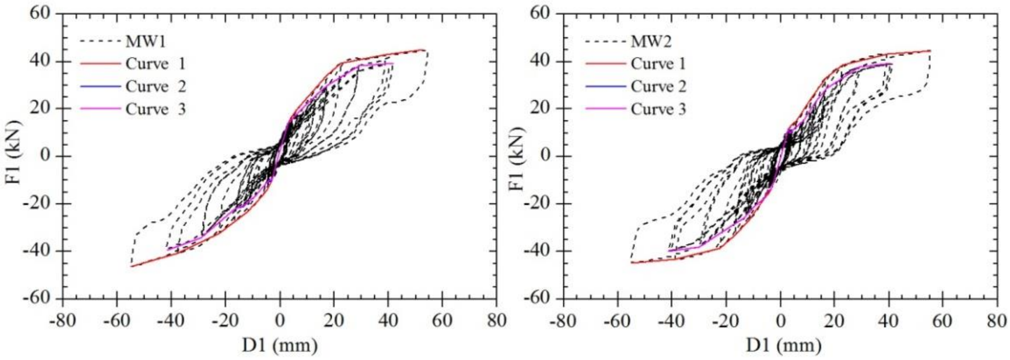

Fig. 15 Force-Displacement curves

Table 4 Wall stiffness

MW1	F_{max} (kN)	F_{min} (kN)	F_{ave} (kN)	$v_{40\%}\,F_{max}$ (mm)	$v_{40\%}\,F_{min}$ (mm)	$v_{40\%}$ (mm)	$v_{10\%}\,F_{max}$ (mm)	$v_{10\%}F_{min}$ (mm)	$v_{10\%}F_{ave}$ (mm)	k (kN/m)
1ª curve	45.1	-55.0	50.1	6.1	-9.1	7.6	0.1	-1.5	0.8	2209.4
2ª curve	39.5	-41.5	40.5	4.5	-9.1	6.8	0.1	-1.5	0.8	2025.4
3ª curve	39.5	-41.5	40.5	4.5	-9.1	6.8	0.1	-1.5	0.8	2025.4
MW2	F_{max} (kN)	F_{min} (kN)	F_{ave} (kN)	$v_{40\%}\,F_{max}$ (mm)	$v_{40\%}\,F_{min}$ (mm)	$v_{40\%}$ (mm)	$v_{10\%}\,F_{max}$ (mm)	$v_{10\%}F_{min}$ (mm)	$v_{10\%}F_{ave}$ (mm)	k (kN/m)
1ª curve	44.8	-55.1	49.9	9.2	-7.2	8.2	0.5	-1.0	0.8	2011.3
2ª curve	39.3	-41.3	40.3	8.7	-5.0	6.9	0.5	-1.0	0.8	1982.8
3ª curve	39.3	-41.3	40.3	8.7	-5.0	6.9	0.5	-1.0	0.8	1982.8

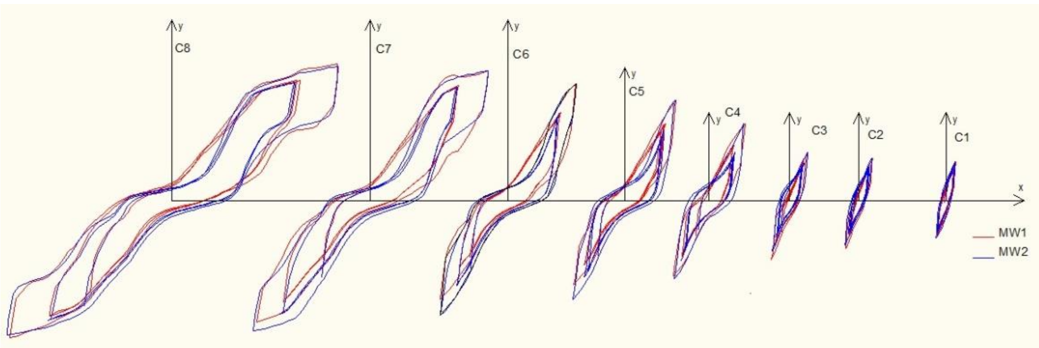

Fig. 16 Energy dissipated in each cycle

Fig. 15 and Table 4 summarize the results need to compute the walls stiffness, estimated in 2015 kN/m in the case of MW1 and 2000 kN/m in the case of MW2 (average of the three curves).

Fig. 16 shows the masonry walls hysteresis cycles along the test. According to Eq. (3) the damping coefficient in each cycle is obtained. In Table 5 the energy dissipated in cycles at different levels of deformation is presented. The increase in deformation leads to an increase in energy dissipation and a decrease in damping, associated to damage in the timber beams and in the masonry infill.

Table 5 Energy dissipated and damping in each cycle

Cycle	MW1						MW2					
	D_{max}. (mm)	F_{max} (kN)	F_{min} (kN)	F_{ave} (kN)	E (kN.mm)	ζ (%)	D_{max}. (mm)	F_{max} (kN)	F_{min} (kN)	F_{ave} (kN)	E (kN.mm)	ζ (%)
C1	3.26	14.42	-10.14	12.28	48.29	19.21	3.05	11.76	-13.66	12.71	58.45	24.00
C2	4.54	17.01	-13.14	15.08	69.30	16.11	4.27	13.36	-15.48	14.42	77.83	20.13
C3	5.94	19.48	-16.21	17.85	97.74	14.68	5.83	15.00	-17.77	16.38	114.59	19.10
C4	11.96	27.50	-23.25	25.38	283.77	14.88	11.41	24.85	-26.88	25.87	312.95	16.87
C5	17.11	34.14	-27.51	30.82	416.15	12.56	16.74	33.32	-36.67	35.00	483.28	13.13
C6	22.45	39.40	-32.47	35.94	610.34	12.04	22.91	38.65	-38.67	38.66	652.44	11.72
C7	39.18	43.06	-40.76	41.91	1377.66	13.35	39.39	43.25	-43.28	43.26	1406.89	13.14
C8	54.40	45.14	-46.43	45.79	2043.75	13.06	55.44	44.78	-44.99	44.88	1984.84	12.70

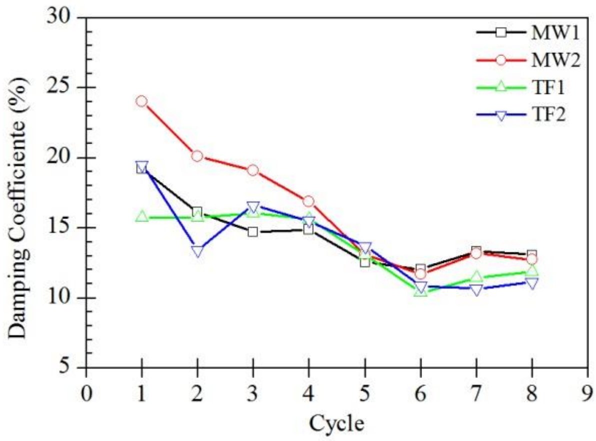

Fig. 17 Damping coefficient in each cycle

(a) Failure by shear of intermediate timber beam in MW1

(b) Failure by longitudinal shear of intermediate timber beam in MW2

Fig. 18 Failure mode of masonry walls.

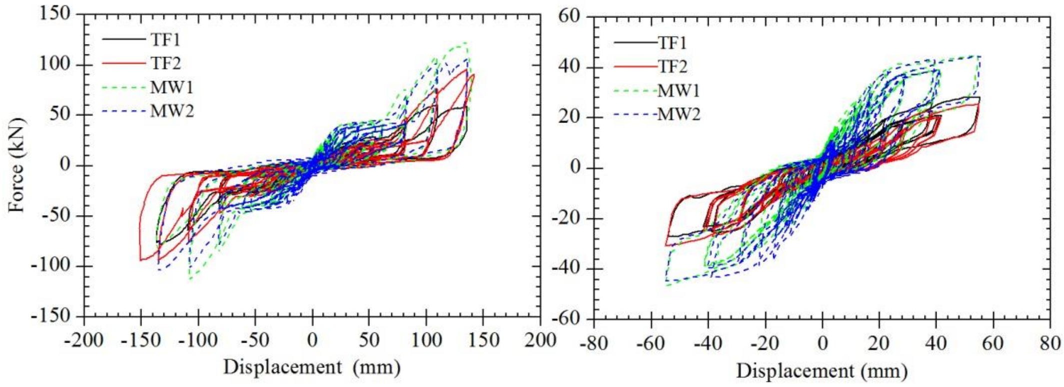

(a) Total displacement

(b) Displacement ±55 mm

Fig. 19 Load-displacement diagrams.

The masonry wall to compared with the timber frames present higher energy dissipation (about the double), which does not occur for damping coefficient are the same values especially for last cycles (Fig. 17).

Figs. 18 (a)-(b) shows the failure modes of the masonry walls. Rupture in MW1 is associated with compression of the diagonals that caused the shear failure of the intermediate beam. In the case of the model MW2 the wall had an early rupture by shear parallel of the timber fibres at one end of the intermediate beam.

3.3 Timber Frames (TF) and Masonry wall (MW)

The load-displacement diagrams obtained for the timber frames (TF) and masonry walls (MW) are shown in Fig. 19(a). Through the analysis of the behaviour in the load-displacement diagrams, an increase in the wall stiffness for displacements higher than 60 mm was observed, associated with the course limit of the vertical jacks. Due to this behaviour, these values cannot be taken into account for the characterization of the walls. Therefore the analysis is limited to a range of ±55 mm displacements as shown in Fig. 19(b).

The hysteretic behaviour of the timber framed wall subjected to cyclic loading is characterized by nonlinear behaviour, with a good ductility response. The maximum strength is 30 kN and 50 kN, for the timber frames and masonry walls respectively, measured at the displacement of 55 mm which results in a 2.6% drift.

As expected, masonry walls exhibited higher average stiffness than timber frames, of 2000 kN/m and 600kN/m respectively. Masonry infill proved to significantly influence the stiffness and especially the strength of the whole module. The masonry infill also influences the collapse mode, namely by preventing the lateral instability of the compressed diagonals.

The masonry walls also have a greater ability to dissipate energy, which implies a larger damping effect, a major relevance parameter regarding the behaviour of the walls subjected to earthquake loading.

4. Conclusions

This paper intended to provide useful information on the cyclic behaviour of traditional timber-framed masonry walls, typical of the Portugal Pombalino buildings and thus to contribute to the state of the art on the issue, given the scarce results available in literature.

The experimental analysis was carried out on two distinct elements of walls, namely timber frame and masonry wall, in order to understand the contribution of each element of the wall. From the experimental campaign carried out it was possible to observe that:

- The damage is highly concentrated at the mortise and tenon connections resulting in the large deformation of the walls. The masonry infill only encountered low damage, mainly at the interface between masonry and timber.
- The masonry walls have a greater ability to dissipate energy, which implies a larger damping effect, a major relevance parameter regarding the behaviour of the walls subjected to earthquake loading.
- Traditional timber-framed masonry walls present high values of ductility, which in average are higher than the ones found in modern timber shear walls. This type of walls present also considerable high values of lateral drift, confirming the capacity for deformation under lateral loads.
- The obtained results enabled the experimental hysteresis curve to be plotted via the relation force-displacement. This shall be useful for the development of analytical models for these walls.

Acknowledgments

The financial support of the Foundation for Science and Technology (FCT) through the research project PTDC/ECM/100168 - REABEPA is acknowledged. The authors also acknowledge HCI for his invaluable help. The laboratory technician Mr. Fernando Alves is also acknowledged for his help in the experimental tests

References

ASTM E2126 (2011), *Standard Test Methods for Cyclic (Reversed) Load Test for Shear Resistance of Vertical Elements of the Lateral Force Resisting Systems for Buildings*, ASTM International, West Conshohocken, PA, 2006, DOI: 10.1520/E2126-11.

Bento, R., Lopes, M. and Cardoso, R. (2005), "Seismic evaluation of old masonry buildings, Part II: analysis of strengthening solutions for a case study", *Eng. Struct.*, **27**, 2014-23.

Cóias e Silva, V., Lourenço, P.B., Ramos, L. and Mesquita, C. (2001), "Accounting for the "block effect" in structural interventions in Lisbon's old "Pombaline" downtown buildings", *Proceedings of the 3rd International Seminar on Historical, Constructions*, Guimarães.

Diskaya, H. (2007), "Damage Assessment of 19th Century Traditional Timber Framed Structures in Istanbul", *From Material to Structure - Mechanical Behaviour and Failures of the Timber Structures, ICOMOS IWC - XVI International Symposium*, Florence, Venice and Vicenza, Italy, November.

Dogangun, A., Tuluk, I.O., Livaoglu, R. and Acar, R. (2006), "Traditional wooden buildings and their damages during earthquakes in Turkey", *Eng. Fail. Anal.*, **13**, 981-996.

Dutu, A., Ferreira, J., Guerreiro, L., Branco, F. and Gonçalves, A. (2012), "Timbered masonry for earthquake resistance in Europe", *Mater. Construcción*, **62,** 615-628.

EN 1991-1-1 (2002), *Eurocode 1: Actions on structures –part 1-1: General actions – Densities, self-weight. Imposed loads for buildings*, Commissions of the European Communities (CEN), Brussels.

EN 338, *Structural Timber*, CEN, 2003.

Ferreira, J.G., Teixeira, M.J., Dutu, A., Branco, F. and Gonçalves, A. (2012), "Experimental evaluation and numerical modelling of timber framed walls", *Exper. Techniq.*, **38**(4), 45-53.

Gonçalves, A., Ferreira, J., Guerreiro, L. and Branco, F. (2011), "Avaliação experimental do comportamento de paredes de edificios pombalinos", *Construlink*, **9**, 52-65.

Gülkan, P. and Langenbach, R. (2004), "The earthquake resistance of traditional timber and masonry dwellings in Turkey", *13th World Conference on Earthquake Engineering*, Vancouver, B.C.

ISO 21581 (2010), *Timber structures - Static and cyclic lateral load test methods for shear walls, New Delhi: Bureau of Indian Standards*, International Organization for Standardization ISO Central Secretariat, Geneva, Switzerland.

Krawinkler, H., Parisi, F., Ibarra, L., Ayoub, A. and Medina, R. (2000), "Development of a testing protocol for wood frame structures", CUREE-Caltech Woodframe Project Rep., Stanford University, Stanford, California.

Langenbach, R. (2007), "From 'Opus Craticium' to the 'Chicago Frame': Earthquake- Resistant traditional construction", *Int. J. Arch. Heritage*, **1**(1), 29-59.

Makarios, T. and Demosthenous, M. (2006), "Seismic response of traditional buildings of Lefkas Island, Greece", *Eng. Struct.*, **28**, 264-278.

Meireles, H. and Bento, R. (2010), "Cyclic behaviour of pombalino frontal walls", *Proceedings of the 14th European Conference on Earthquake Engineering (14ECEE)*, Ohrid, F.Y.R.O. Macedonia.

Redondo, E.G., and Hernández-Ros, R.A. (2003), "Wooden framed structures in Madrid domestic architecture of 17th to 19th centuries", *Proceedings of the First International Congress on Construction History*, Madrid, January.

Santos, P. (1997), "Ensaios de Paredes Pombalinas", Nota técnica N 15/97, NCE/DE, LNEC, Lisbon.

Santos, P. (1999), "Laboratory Tests on Masonry walls taken from an Ancient Building in Lisbon", *Proc. of the 34th Meeting of CIB W023 Comission in October 1997 in Lisbon*, **231**, CIB Publication, Lisbon.

CC